

Improved Dutch Roll Approximation for Hypersonic Vehicle

^{1,*} Liang-Liang Yin, ¹ Yi-min Huang, ¹ Chun-Zhen Sun,
² Jie Jia, ^{3,*} Yong Yang

¹ College of Automation Engineering, Nanjing University of Aeronautics and Astronautics,
Nanjing, 210016, China

² College of Information Engineering, Nanchang Hangkong University, Nanchang, 330069, China

³ School of Information Technology, Jiangxi University of Finance and Economics,
Nanchang 330013, China

* E-mail: yinliangshmily@126.com

Received: 18 April 2014 /Accepted: 31 May 2014 /Published: 30 June 2014

Abstract: An improved dutch roll approximation for hypersonic vehicle is presented. From the new approximations, the dutch roll frequency is shown to be a function of the stability axis yaw stability and the dutch roll damping is mainly effected by the roll damping ratio. In additional, an important parameter called roll-to-yaw ratio is obtained to describe the dutch roll mode. Solution shows that large-roll-to-yaw ratio is the generate character of hypersonic vehicle, which results the large error for the practical approximation. Predictions from the literal approximations derived in this paper are compared with actual numerical values for s example hypersonic vehicle, results show the approximations work well and the error is below 10 %. *Copyright © 2014 IFSA Publishing, S. L.*

Keywords: Hypersonic vehicle, Dutch roll, Literal approximation, Roll-to-yaw ratio.

1. Introduction

Dutch roll is an oscillatory interchange between side slip, roll and yaw that occurs as a statically stable aircrafts to reestablish lateral and directional equilibrium [1-3]. It is usually the most complex mode of an aircraft.

Dutch roll is characterized by the frequency and damping, which can be easily done by numerically determining the eigenvalues and eigenvectors associated with the linearized equations of motion [4-7]. However, the eigenvalues and eigenvectors for dutch roll depend on many parameters, and the nature of this dependence is not easily observable from a numerical solution. For this reason, a literal-form approximation is desired to

evaluate the dutch roll. In addition, a literal-form solution has always been useful for the optimization of flight control system.

Literal approximation to the dutch roll has traditionally been derived by considering simplifying assumptions [8, 9]. The approximation has been described in several textbooks and has been widely used over the past several decades [10-13]. However, results obtained from the traditional approximation are not in particularly good agreement with the numerical solution for hypersonic vehicle, which flight with high angle of attack and large mach numbers [14, 15].

In this paper, an improved dutch roll literal approximation for hypersonic vehicle is presented. In addition, a parameter called roll-to-yaw ratio is

obtained to describe the mode, which scaled the relative amplitudes between roll rate and yaw rate. Solution shows that most of the hypersonic vehicles have large roll-to-yaw ratio character, because of the high angle of attack and slender shape. The paper also point out that the large roll-to-yaw ratio is the mainly reason for the poor agreement between traditional appropriate and numerical solution. Finally, predictions from the improved literal approximation are compared with actual numerical values for an example hypersonic vehicle. The result indicates the improved approximation works well and the errors for dutch roll frequency, damping and roll-to-yaw ratio are all within 10 %.

2. Lateral-Directional Dynamics for Hypersonic Vehicle

The lateral-directional equations of motion for hypersonic vehicle are well defined for the form

$$\Delta \dot{x} = A \Delta x, \quad (1)$$

where Δx is the perturbed state vector,

$$\Delta x = [\Delta \beta, \Delta \phi, \Delta p, \Delta r]^T, \quad (2)$$

The lateral-directional system matrix is given by Eq. (3).

$$A = \begin{bmatrix} \frac{Y_\beta}{V} & \frac{g}{V} & \frac{Y_p}{V} + \sin \alpha_0 & \frac{Y_r}{V} - \cos \alpha_0 \\ 0 & 0 & 1 & \tan \alpha_0 \\ L'_\beta & 0 & L'_p & L'_r \\ N'_\beta & 0 & N'_p & N'_r \end{bmatrix}, \quad (3)$$

The characteristic equation for this system can be written as in terms of eigenvalues as

$$|sI - A| = (s - \lambda_r)(s - \lambda_s)(s^2 + 2\xi_{DR}\omega_{DR} + \omega_{DR}^2), \quad (4)$$

where λ_r is the pole of roll mode, λ_s is the pole of spiral mode, ω_{DR} is the dutch roll frequency and ξ_{DR} is dutch roll damping. Dutch roll is the most important and complex mode in these three modes and the traditional dutch roll approximation can be found in many textbooks on flight dynamics to be

$$\omega_d = \sqrt{N'_\beta + (Y_\beta/V)N'_r}, \quad \xi_d = \frac{-N'_r - Y_\beta/V}{2\omega_d} \quad (5)$$

This dutch roll approximation has been used in practical application for the past several decades. (about UAV supersonic vehicle). However It is quite apparent from Table 3, that the approximation is rather inaccurate for both ω_{DR} and ξ_{DR} for hypersonic vehicle.

3. Improved Dutch Roll Approximation for Hypersonic Vehicle

The traditional approximation for dutch roll is obtained by neglecting the rolling rate. The assumption is reasonable for low speed aircrafts, which have big wingspan and dutch roll amplitude for the rolling rate is smaller than that for the yawing rate. However, for hypersonic vehicles, which usually have slender body and flight with high angle of attack, dutch roll amplitude for the rolling rate is much larger than the yawing rate. In this section, we develop a parameter called roll-to-yaw ratio, which is defined as the ratio of the amplitudes of the rolling rate and yawing rate in dutch roll. Results show that hypersonic vehicle usually have big roll-to-yaw ratio and the rolling rate could not be neglected. To increase the precision for dutch roll, we develop an improved dutch roll approximation that includes the effects of rolling rate.

4.1. Dutch roll Frequency ω_{DR}

For dutch roll frequency approximation, we neglect the gravity and damping term, because these values are little and have little effect on dutch roll frequency. Hence, the lateral-directional system matrix can be written as

$$A = \begin{bmatrix} \frac{Y_\beta}{V} & 0 & \sin \alpha_0 & -\cos \alpha_0 \\ 0 & 0 & 1 & \tan \alpha_0 \\ L'_\beta & 0 & 0 & 0 \\ N'_\beta & 0 & 0 & 0 \end{bmatrix}, \quad (6)$$

The characteristic equation becomes

$$|sI - A| = s^2 \left(s^2 - \frac{Y_\beta}{V}s + N'_\beta \cos \alpha_0 - L'_\beta \sin \alpha_0 \right), \quad (7)$$

Here we have lost two roots, one resulting from the assumption of no gravity and the other resulting from the assumption of no damping terms (the spiral and rolling modes, respectively).

From Eq. 4 and Eq. 7, the dutch roll frequency is

$$\omega_{DR} = \sqrt{N'_\beta \cos \alpha_0 - L'_\beta \sin \alpha_0}, \quad (8)$$

From Eq. 7, the requirements for lateral-directional static stability is

$$N'_\beta \cos \alpha_0 - L'_\beta \sin \alpha_0 > 0, \quad (9)$$

If we neglected the product of inertia I_{xz} , the Eq. 9 can be reduces to the equivalent condition.

$$C_{n,dyn}^\beta > 0, \quad (10)$$

where

$$C_{n,dyn}^\beta = C_n^\beta \cos \alpha_0 - \frac{I_{zz}}{I_{xx}} C_l^\beta \sin \alpha_0, \quad (11)$$

Equation 11 indicates that $C_{n,dyn}^\beta$ is directly related to the generalized static stability requirement, and the traditional lateral-directional stability criterion C_n^β is only valid when $\alpha_0 = 0$.

4.2. Roll-to-Yaw Ratio $\left| \frac{p}{r} \right|_{DR}$

Roll-to-yaw ratio is defined as the ratio of the amplitudes of the rolling rate and yawing rate in dutch roll mode. For aircrafts with low roll-to-yaw ratio, yawing motion is much larger than rolling motion and vice versa. Roll-to-yaw ratio is equal to the ratio of rolling rate and yawing rate in eigenvector associate with dutch roll mode. The lateral-directional eigenvectors is given by Table 1.

Table 1. The lateral eigenvectors.

	Roll mode	Spiral mode	Dutch roll mode	
β	v_{11}	v_{12}	v_{13}	v_{14}
ϕ	v_{21}	v_{22}	v_{23}	v_{24}
p	v_{31}	v_{32}	v_{33}	v_{34}
r	v_{41}	v_{42}	v_{43}	v_{44}

Thus,

$$\left| \frac{p}{r} \right|_{DR} = \left| \frac{v_{34}}{v_{44}} \right|, \quad (12)$$

The ratio of the x_i and x_j elements in the eigenvector associated with mode k have been denoted by

$$\left(\frac{x_i}{x_j} \right)_{\text{modek}} = (-1)^{i-j} \left| \frac{\Delta_{qi}(s)}{\Delta_{qj}(s)} \right|_{s=\lambda_k}, \quad (13)$$

where $\Delta_{qi}(s)$ and $\Delta_{qj}(s)$ are the minors of the characteristic determinant of the system. Thus,

$$\left(\frac{p}{r} \right)_{DR} = -\frac{\Delta_{43}}{\Delta_{44}} \Big|_{s=-\xi_{DR}\omega_{DR} + j\omega_d \sqrt{a-\xi_{DR}^2}}, \quad (14)$$

Neglect the terms $\frac{Y_p}{V}$, $\frac{Y_r}{V}$ and L'_r , characteristic determinant of the system becomes

$$|sI-A| = \begin{bmatrix} s-Y'_\beta & -\frac{g}{V} & -\frac{Y'_p}{V} \sin \alpha & -\frac{Y'_r}{V} \cos \alpha \\ 0 & s & -1 & 0 \\ -L'_\beta & 0 & s-L'_p & 0 \\ -N'_\beta & 0 & -N'_p & s-N'_r \end{bmatrix}, \quad (15)$$

$\Delta_{qi}(s)$ and $\Delta_{qj}(s)$ can be obtained by

$$\Delta_{43} = - \begin{vmatrix} s & 0 & \cos \alpha \\ 0 & s & \tan \alpha_0 \\ -L'_\beta & 0 & 0 \end{vmatrix} = -sL'_\beta \cos \alpha, \quad (16)$$

and

$$\Delta_{44} = \begin{vmatrix} s & 0 & -\sin \alpha \\ 0 & s & -1 \\ -L'_\beta & 0 & s-L'_p \end{vmatrix} = s(s-L'_p) - L'_\beta \sin \alpha, \quad (17)$$

Thus,

$$\begin{aligned} \left(\frac{p}{r} \right)_{DR} &= \left| \frac{-L'_\beta \cos \alpha}{s(s-L'_p) - L'_\beta \sin \alpha} \right|_{s=-\xi\omega_d + j\omega_d \sqrt{1-\xi^2}} \\ &= \left| \frac{L'_\beta \cos \alpha}{2\xi^2 \omega_d^2 - \omega_d^2 + \xi\omega_d L'_p - L'_\beta \sin \alpha - j\omega_d \sqrt{1-\xi^2} (2\xi\omega_d + L'_p)} \right| \end{aligned} \quad (18)$$

The roll-to-yaw ratio is defined by the amplitudes of $\left(\frac{p}{r} \right)_{DR}$ as follows

$$\begin{aligned} \left| \frac{p}{r} \right|_{DR} &= \left| \frac{L'_\beta \cos \alpha}{\sqrt{(2\xi^2 \omega_d^2 - \omega_d^2 + \xi\omega_d L'_p - L'_\beta \sin \alpha)^2 + (\omega_d \sqrt{1-\xi^2} (2\xi\omega_d + L'_p))^2}} \right| \\ &= \left| \frac{L'_\beta \cos \alpha}{\sqrt{(\omega_d^2 + L'_\beta \sin \alpha)^2 + \omega_d^2 L_p^2}} \right| \end{aligned} \quad (19)$$

From Eq. 8 and Eq. 19, the roll-to-yaw ratio is

$$\left| \frac{p}{r} \right|_d = \frac{L'_\beta}{N'_\beta} \frac{1}{\sqrt{1 + \frac{L_p^2}{N'_\beta \cos \alpha} - \frac{L'_\beta \sin \alpha L_p^2}{N_\beta^2 \cos^2 \alpha}}}, \quad (20)$$

The roll-to-yaw ratio is mainly effected by the ratio of lateral static stability and directional static stability in stability axes. Directional static stability of hypersonic vehicles is usually weak, for the vertical stabilizer being shaded by the body at high angle of attack. In addition, the hypersonic vehicle most has a slender shape. Hence, the roll-to-yaw ratio is very large. Results from Table 2 indicate that the

roll-to-yaw ratio of a hypersonic vehicle reaches as large as 15 when the AOA reaches 30. This also points out why the traditional approximation is not satisfactory for hypersonic vehicle.

4.3. Dutch roll Damping ξ_{DR}

For the large roll-to-yaw ratio, dutch roll of a hypersonic vehicle consists mainly of sideslipping and rolling, and the yawing contributes little to the dutch roll. With neglecting the yawing rate, we lead to a three-degrees-of-freedom dutch approximation. The simplified third-order system matrix is as follows.

$$A = \begin{bmatrix} \frac{Y_\beta}{V} & \frac{g}{V} & \sin \alpha_0 \\ 0 & 0 & 1 \\ L'_\beta & 0 & L'_p \end{bmatrix}, \quad (21)$$

The characteristic polynomial is now obtained very easily by the system matrix

$$|sI - A| = s^3 - s^2(L'_p + \frac{Y_\beta}{V}) + s(L'_p \frac{Y_\beta}{V} + L'_\beta \sin \alpha_0) - L'_\beta \frac{g}{V}, \quad (22)$$

This polynomial has a root correspond to the roll subsidence pole and two quadratic roots correspond to the dutch roll poles. Hence, the polynomial could be written as

$$|sI - A| = (s^2 + 2\xi_{DR}\omega_{DR}s + \omega_{DR}^2)(s - \lambda_r), \quad (23)$$

From Eq. 22 and Eq. 23, we obtain

$$\begin{cases} 2\xi_{DR}\omega_{DR} + d = -L'_p - \frac{Y_\beta}{V} \\ \omega_{DR}^2 \cdot d = -L'_\beta \frac{g}{V} \end{cases}, \quad (24)$$

According to Eq. 8 and Eq. 24, the dutch roll frequency and damping is given by

$$\begin{cases} \omega_{DR} = \sqrt{N'_\beta \cos \alpha - L'_\beta \sin \alpha} \\ \xi_{DR} = -\frac{L'_p}{2\omega_{DR}} - \frac{Y_\beta}{2\omega_{DR}V} + \frac{L'_\beta g}{2\omega_{DR}^3 V} \end{cases}, \quad (25)$$

The expression indicates that the dutch roll damping is dominated by the derivative L'_p (V is very large for hypersonic vehicle), which is the behavior of aircrafts with large roll-to-yaw ratio. The damping formula tends to be more accurate than traditional approximation. This will be illustrated later, by example.

The damping formula is helpful for stability argument of dutch roll. For a conventional aircraft, it is effective to increase the dutch roll damping by

feeding back yawing rate to rudder, which increases N'_r as given by Eq. 6. However, for a hypersonic vehicle, it will be more effective to feed back rolling rate to aileron, which to increase L' as given by Eq. 25.

5. Numerical Illustration

As an illustration, predictions from the dutch roll approximation in this paper are now compared with exact numerical values for an example hypersonic vehicle. Consider the aircraft at $\alpha = 30^\circ$ and $H = 70\text{km}$ having

$$V = 7000, \quad L_\beta = -9.63, \quad N_\beta = -0.12$$

$$L_p = 5.6 \times 10^{-3}, \quad L_r = 1.39 \times 10^{-3}, \quad N_p = -4.45 \times 10^{-4}$$

$$N_\beta = -5.6 \times 10^{-4}, \quad Y_\beta = 2.83 \times 10^{-4}, \quad Y_p = 0.64$$

$$Y_\beta = -0.76$$

For this aircraft and flight condition, the exact numerical solution obtained numerically from the linearized equation of motion gives

$$\left| \frac{p}{r} \right|_{DR} = 14.3, \quad \omega_{DR} = 1.16, \quad \xi_{DR} = -9.7 \times 10^{-4}$$

The approximate solution obtain by using Eq. 20 and Eq. 25 results in

$$\left| \frac{p}{r} \right|_{DR} = 14.5, \quad \omega_{DR} = 1.16, \quad \xi_{DR} = -1.0 \times 10^{-3}$$

From the above results, the roll-to-yaw ratio, frequency and damping predicted by the improved dutch roll approximation agree very closely with the exact solution. The roll-to-yaw error is by 2 %, the frequency error is by 2 % and the damping error is by 5 %.

Table 2 and Table 3 give the compared results between the improved approximation and the traditional approximation, with the angle of attack varying between 17 and 30 degrees, the altitude varying between 85 and 55 km and the mach numbers varying between 22 and 17.

Table 2. Comparing of roll-to-yaw ratio to numerical values.

H, α, M_a	Numerical solution	Approximate solution	Error
(85,30,22)	17.7	17.5	1.2 %
(77,30,21)	16.4	16.5	0.6 %
(70,30,20)	14.3	14.2	0.7 %
(65,25,19)	9.0	9.1	1.1 %
(60,25,18)	7.6	7.5	1.3 %
(55,20,17)	5.5	5.5	0.0 %

Table 3. Comparing of dutch roll to numerical values.

Flight Condition	Dutch Roll Frequency					Dutch Roll Damping						
	Numerical solution	Improve Approximation		Traditional Approximation		Numerical solution	Improve Approximation		Traditional Approximation			
		value	error	value	error		value	error	value	error		
H, α, M_a	value		value	error	value	error	value		value	error		
(85,30,22)	0.66		0.66	0.0	0.21	67.9	-1.75×10^{-3}		-1.8×10^{-3}	2.8	-7.7×10^{-5}	95.6
(77,30,21)	1.16		1.16	0.0	0.38	66.8	-9.7×10^{-4}		-1.0×10^{-3}	3.1	-1.3×10^{-4}	86.5
(70,30,20)	1.56		1.56	0.0	0.55	64.7	-7.0×10^{-4}		-7.3×10^{-4}	4.3	-1.7×10^{-4}	76.1
(65,25,19)	1.86		1.86	0.0	0.85	54.0	-5.8×10^{-4}		-6.1×10^{-4}	5.2	-5.3×10^{-5}	90.1
(60,25,18)	2.50		2.50	0.0	1.22	50.8	-3.4×10^{-4}		-3.2×10^{-4}	5.5	-5.6×10^{-5}	83.7
(55,20,17)	2.76		2.76	0.0	1.64	40.5	-3.3×10^{-4}		-3.1×10^{-4}	6.2	-1.0×10^{-4}	68.9

Table 2 shows how the roll-to-yaw ratio given by Eq. 20 compares with the exact numerical solution for a broad range of flight condition. It indicates that the approximate roll-to-yaw ratio given by Eq. 20 is in good agreement with the exact solution. In addition, as the angle of alpha grows, the roll-to-yaw ratio becomes more and more large. This is because the vertical stabilizer is shaded by the body and the directional static stability is low as the alpha increases.

A comparison of the improved dutch roll approximation with the exact numerical values is shown in Table 3, which also contains a comparison of the traditional approximation. Clearly, the improved approximation seems to predict the actual values well, and is definitely superior to the traditional approximation. The frequency error is by 2 % and the damping error is by 6 %.

Note that, with the decrease in angle of attack, the damping error for the improved dutch roll approximation increases. This is because the roll-to-yaw ratio decreases as the angle of attack decreases. As the roll-to-yaw ratio is lower, the improved approximation becomes worse, which base on a large roll-to-yaw ratio. For example, if we decouple the N'_β in the earlier example, the aircraft becomes a small roll-to-yaw ratio type. In this case, the exact numerical values is

$$\xi_{DR} = -1.0 \times 10^{-3}$$

The approximate values by Eq. 25 is

$$\xi_{DR} = -1.0 \times 10^{-3}$$

We found that, the error will increase to 50 % when the roll-to-yaw ratio is less than 2.0. Nevertheless, nearly all hypersonic vehicles have roll-to-yaw ratio more than 2.0.

6. Conclusions

An improved dutch roll approximation for hypersonic vehicles has been developed. The traditional dutch roll approximation neglects the

rolling rate, which is valid only for aircrafts with small roll-to-yaw ratio. However, hypersonic vehicles are a classical type of aircrafts with large roll-to-yaw, for which the traditional approximation is invalid. The improved dutch roll approximation considers the effect of rolling rate, and has higher accuracy as the roll-to-yaw ratio increases. Results show that the improved dutch roll approximation works well under a wide range of flight conditions.

Acknowledgements


This work was supported by the Fundamental Research Fund (56XZA12008), by the National Natural Science Foundation of China (61263012, 61263040), by the Postdoctoral Foundation of China (2012M510593), by the Aerospace Science Foundation (20120156001), by the Natural Science Foundation of Jiangxi Province (20114BAB211020, 20132BAB201025), by the Young Scientist Foundation of Jiangxi Province (20122BCB23017), and by the Science and Technology Research Project of the Education Department of Jiangxi Province (No. GJJ13302).

References

- [1]. L. Huang, Z. S. Duan and J. Y. Yang, Challenges of control science in near space hypersonic aircrafts, *Control Theory & Applications*, Vol. 28, October 2011, pp. 1496-1505.
- [2]. N. M. Qi, Q. H. Zhou and C. M. Qin, The Six DOF Model of Hypersonic Vehicle and Coupling Characterization Analysis, *Journal of Projectiles, Rockets, Missiles and Guidance*, Vol. 32, 2012, pp. 49-52.
- [3]. Philip Calhoun, An entry flight controls analysis for a reusable launch vehicle, in *Proceedings of the 38th Aerospace Sciences Meeting and Exhibit*, 2000.
- [4]. M. T. Moul, J. W. Paulson, Dynamic Lateral Behavior of High-Performance Aircraft, *NASA*, RM-L58E16, 1958.
- [5]. D. Siqueira, P. Paglione and F. Moreira, Robust fixed structure output feedback flight control law synthesis and analysis using singular structured value, *Aerospace Science and Technology*, Vol. 30, 2013, pp. 102-107.

- [6]. W. Wang and P. P. Menon, Bates D G, et al., Robustness analysis of attitude and orbit control systems for flexible satellites, *IET Control Theory and Applications*, Vol. 4, 2010, pp. 2958-2970.
- [7]. A. Gruszka, M. Malisoff and F. Mazenc, Bounded Tracking Controllers and Robustness Analysis for UAVs, *IEEE Transactions on Automatic Control*, Vol. 58, 2013, pp. 180-187.
- [8]. H. P. Lee, M. Chang and M. K. Kaiser, Flight dynamics and stability and control characteristics of the X-33 technology demonstrator vehicle, in *Proceedings of the Guidance, Navigation, and Control Conference and Exhibit*, 1998, AIAA-98-4410.
- [9]. L. N. Wu, Y. M. Huang and C. L. He, Reusable Launch Vehicle Lateral Control Design of Glide Return Phase, *Journal of Nanjing University of Aeronautics and Astronautics*, Vol. 41, 2009, pp. 329~333.
- [10]. Ridwan Kureemun, Declan Bates, Martin Hayes, On the generation of LFT-based uncertainty models for flight control law robustness analysis, in *Proceedings of the AIAA Guidance, Navigation, and Control Conference and Exhibit*, 2001, AIAA-2001-4396.
- [11]. K. Y. Tu, A. Sideris, K. D. Mease and J. Nathan, Robust lateral-directional control design for the F/A-18, in *Proceedings of the Guidance, Navigation, and Control Conference and Exhibit*, 1999, AIAA-99-4204.
- [12]. I. Gregory, J. McMinn and J. Shaughnessy, Hypersonic vehicle control law development using H^∞ and μ -synthesis, in *Proceedings of the 4th Symposium on Multidisciplinary Analysis and Optimization*, 1992, AIAA-1992-5010.
- [13]. L. Liu, Advanced Verification and Clearance Techniques for Modern Flight Control Systems, *National Defense Industry Press*, Beijing, 2010, pp. 52-58.
- [14]. B. Morton, R. McAfoos, A μ -test for real parameter variations, in *Proceeding of the ACC*, 1985, pp. 135-138.
- [15]. G. Ferreres, A practical approach to robustness analysis with aeronautical applications, *Kluwer Academic/ Plenum Publishers*, New York, 1999.

2014 Copyright ©, International Frequency Sensor Association (IFSA) Publishing, S. L. All rights reserved.
(<http://www.sensorsportal.com>)



Universal Sensors and Transducers Interface (USTI-EXT) for extended temperature range

-55 °C ... +150 °C

26 measuring modes for all frequency-time parameters, rotational speed, capacitance Cx, resistance Rx, resistive bridges
Frequency range, 0.05 Hz ... 7.5 MHz (120 MHz);
Programmable relative error, % 1 ... 0.0005 %
Conversion speeds 6.25 us ... 12.5 ms
SPI, I2C, RS232 (master and slave, up to 76 800 baud rate)
Packages: 32-lead, 7x7 mm TQFP and 32-pad, 5x5 mm (QFN/MLF)

Applications: automotive industry, avionics, military, etc.

<http://www.techassist2010.com/> info@techassist2010.com